TECHNICAL TRANSACTIONS | CZASOPISMO TECHNICZNE
MECHANICS | MECHANIKA
2-M/2016

ANDRZEJ DUDA, JERZY KAMIEŃSKI*

THE CIRCULATION OF LIQUID IN THE MIXING VESSEL EQUIPPED WITH DIFFERENT DUAL IMPELLERS

CYRKULACJA CIECZY W APARACIE Z DWOMA RÓŻNYMI MIESZADŁAMI

Abstract

The aim of the article was the analysis of liquid flow of radial-axial circulation in the mixing vessel equipped with a dual impeller set, of which the lower impeller induces radial-axial liquid stream, while the upper is turbine disc impeller with vertical blades, ejecting the liquid radially. On the basis of measurements of the liquid instantaneous velocity, the circulation flow rate was evaluated and supplemented with the exchange flow rate – occurring between adjacent compartments. The usage of a CMA model allows to describe the cycle of liquid transport.

Keywords: mixing, circulation of liquid,

Streszczenie

W artykule analizowano przepływy strumieni cieczy cyrkulacji promieniowo-osiowej w zbiorniku z dwoma mieszadłami na wale, z których dolne wytwarza promieniowo-osiowy strumień cieczy, górnym zaś jest mieszadło turbinowe tarczowe, z pionowymi łopatkami, wyrzucającymi ciecz promieniowo. W oparciu o pomiary chwilowej prędkości cieczy wyznaczono wydatek jej przepływu cyrkulacyjnego, uzupełniony o przepływy między obszarami cyrkulacyjnymi. Korzystając z modelu CMA opisano cykl przenoszenia cieczy.

Słowa kluczowe: mieszanie, curkulacja cieczy

DOI:

* MSc. Eng. Andrzej Duda, Firma Doradczo-Inżynieryjna EDA, Wieliczka, Prof. PhD. DSc. Eng. Jerzy Kamieński, Institute of Thermal and Process Engineering, Faculty of Mechanical Engineering, Cracow University of Technology.

1. Introduction

This study is dedicated to the flows of liquid streams of the radial-axial circulation in a mixing vessel equipped with different dual impeller sets. In each dual set, the lower impeller induces radial-axial liquid stream, while the upper is a turbine disc impeller with vertical blades, ejecting the liquid radially.

The impellers, rotating in the liquid, spin it as a stream of primary circulation. Whereas the centrifugal force acting on the spinning liquid induces secondary circulation in the entire volume of the vessel. This secondary circulation is known as radial-axial circulation and is related to the pumping process of the impellers. This circulation is crucial for proper and efficient mixing.

In order to achieve the required intensity of the mixing process, two impellers are often assembled on a common drive shaft. Such solution is often used in the mixing of a multiphase systems.

The paper presents the study on three dual impeller sets, located on a common single shaft, at several different distances from each other. During the experiments, the values of the instantaneous velocity of liquid were measured (radial and axial component of the velocity). Then, on the basis of the mean velocities, the circulation flow rate of the liquid was determined.

In the study, the Compartment Model Approach (CMA) was used. The total flow rate values were supplemented by the exchange flow rate of the liquid occurring between circulation compartments. This additional flow rates are caused by fluctuations of liquid velocity. Based on the CMA model, the two-dimensional chart of liquid transport in an apparatus was described. Further use of this model enabled to describe the cycle of liquid transport in an apparatus, the duration of which was related to the mixing time, and could be a measure of the mixing process efficiency when considered it together with energy consumption.

2. Experimental set-up and methodology

The measurements of the instantaneous velocities of liquid were performed using two-channel laser Doppler anemometer (LDA, delivered by the DANTEC Company), operating in the backscattering mode [6]. The experiments were carried out in a cylindrical vessel, with the inner diameter of D = 0.286 m, equipped with four flat baffles, each with the standard width of $0.1 \cdot D$. The cylindrical vessel was built in the rectangular jacket. Both of them were made of the same material, a borosilicate glass of the DURAN type. To eliminate an error of the refraction effect, occurring when the laser beams pass through different materials, the dimethyl sulfoxide, fully transparent liquid, having the same refractive index as DURAN glass, was employed in the experiments. The temperature of the liquid and vessels' walls was controlled by the thermostatic system; the measurements were carried out at the temperature of 22.5°C, wherein the density of the dimethyl sulfoxide was 1100 kg/m^3 and the dynamic viscosity coefficient – of 2.3 mPa.

As the seeding particles, the hollow glass spheres with a silver plated outer surface (trade symbol S-HGS) were used in the experiments. The mean diameter of the particles

was 10 μm, and their average density was 1150 kg/m^3. Both the vessel and the jacket were filled up with liquid to the height of 1.258*D*.

Three different dual impeller sets were examined. The upper impeller was in each case the disc turbine, equipped with six vertical, flat blades – TR-6. The lower impeller was exchanged by three different types: the turbine with six blades inclined at 45° (Pitched Blade Turbine, PBT-6 type), the hydrofoil Chemineer HE-3 impeller [4] and the hydrofoil Lightnin A-315 impeller [12]. The diameter of all examined impellers was of $d = D/3$. The lower impeller was in each case located at the distance of $h = 0.5 \cdot d$ from the vessel's bottom and the value of the impeller spacing Δh was changed in the range of $(0.5 \div 2) \cdot d$.

The liquid velocities were measured in the selected points, located at the vertical middle plane of the vessel, placed between two successive baffles and forming a regular, rectangular grid. The measurement points were spaced by 0.005 m along the radius of the vessel and its height. The two components of the instantaneous velocity of liquid were measured: the radial $u_r(t)$ and the axial $u_z(t)$.

The experiments were carried out within the turbulent flow regime of liquid, at a constant rotational frequency of impellers of 5 [s^{-1}], which corresponded to the Reynolds number for a mixing process, $Re \approx 2.16 \cdot 10^4$. The power consumption was an additional magnitude measured during the experiments.

3. Experimental results

3.1. Mean velocities of liquid

The values of the velocity components: mean $\bar{u}$ and fluctuating u', were calculated on the basis of prior measurement data of the instantaneous velocities, benefiting from the FLOware software.

The components of mean velocity $\bar{u}_i$ were calculated as the weighted averages, with weights corresponding to the residence time $\Delta t_{i,j}$ of seeding particles in the measurement volume [6, 11]:

$$\bar{u}_i = \frac{\sum_{i=1}^{N} u_{i,j} \cdot \Delta t_{i,j}}{\sum_{i=1}^{N} \Delta t_{i,j}} \tag{1}$$

The shape and intensity of the mean flow of liquid in the mixing vessel is determined by the distributions of velocity components and their local values. The primary circulation of liquid, induced during the mixing process by rotating impellers, is partly being converted to the secondary, related to the radial-axial flow. This flow is also directly related to the components of mean velocity: radial and axial.

These radial-axial flows of liquid, occurring in the mixing vessel, depend on the design of applied impellers and their mutual position. They were illustrated in Figs. 1÷3, as distributions of the resultants of mean velocities in the radial and axial direction. They were drawn at the vertical middle plane located between two baffles in the vessel.

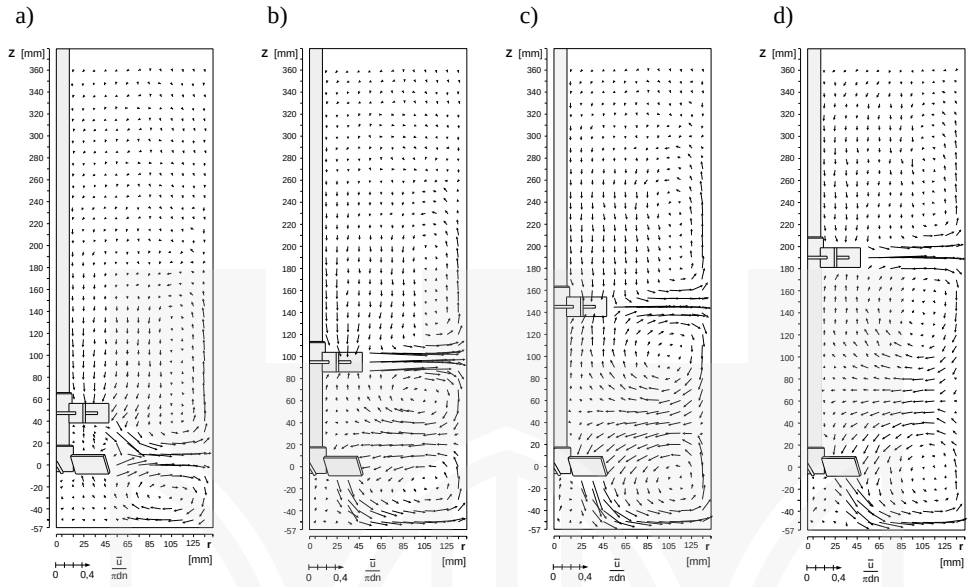

Fig. 1. The distribution of the resultants of mean liquid velocities in the radial and axial direction, in the dual mixing vessel equipped with the upper disc turbine TR-6 and the lower impeller pitched blade turbine PBT-6. The impeller spacing:a) $\Delta h = 0.5d$, b) $\Delta h = d$, c) $\Delta h = 1.5d$, d) $\Delta h = 2d$ [5]

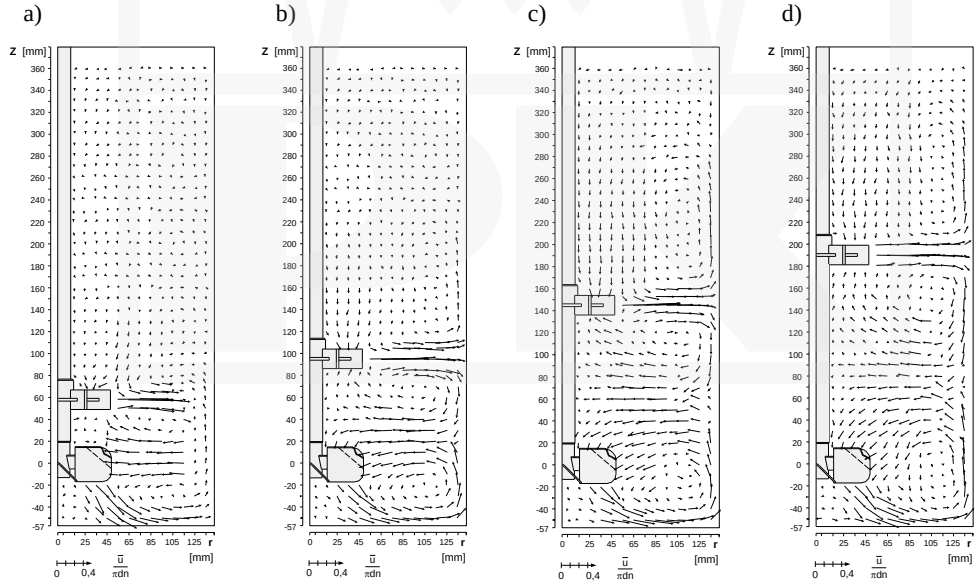

Fig. 2. The distribution of the resultants of mean liquid velocities in the radial and axial direction, in the dual mixing vessel equipped with the upper disc turbine TR-6 and the lower A-315 impeller; the impeller spacing: a) $\Delta h = 0.6d$, b) $\Delta h = d$, c) $\Delta h = 1.5d$, d) $\Delta h = 2d$ [5]

All examined dual impeller sets induce an advantageous structure of the liquid flow in the mixing vessel. When the impellers are at sufficient distance, the flow of liquid is expanded in the entire volume and is sufficiently intense. The flow structure is then composed of several compartments, close to the model structure of a multistage mixing [1, 15, 18]. The circulation flows in the mixing vessel are similar; however, they differ from each other quantitatively, depending on the design of the lower impeller.

The adjacent circulation loops interact only at certain distances between the impellers. If these distances are too small or too large, then the interaction completely disappears. At small values of the spacing, the adjacent circulation loops induced by the upper and the lower impeller coalesce into one common. The shapes of these loops are determined by the resultant streams of the liquid flow, pumped through both of the impellers.

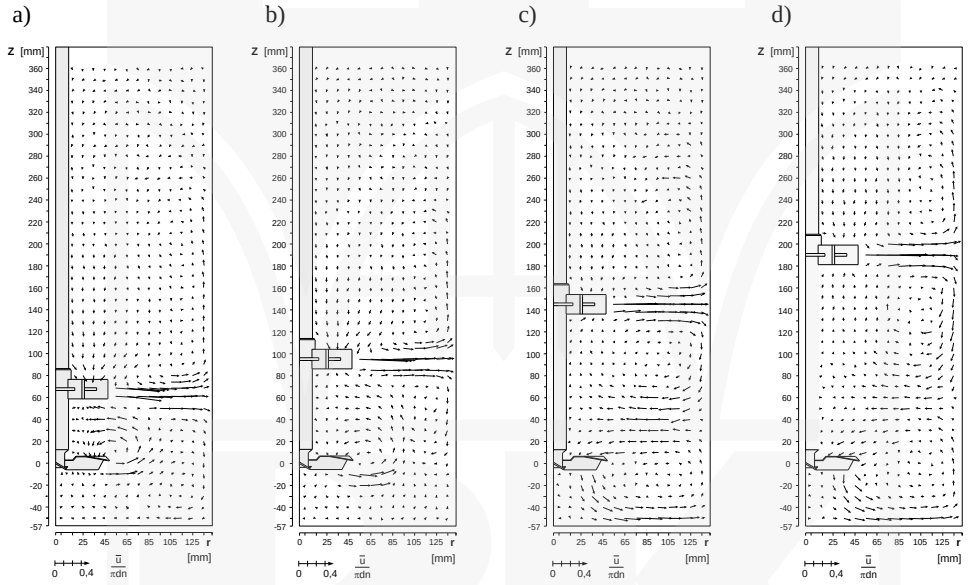

Fig. 3. The distribution of the resultants of mean liquid velocities in the radial and axial direction, in the dual mixing vessel equipped with the upper disc turbine TR-6 and the lower HE-3 Impeller; the impeller spacing: a) $\Delta h = 0.7d$, b) $\Delta h = d$, c) $\Delta h = 1.5d$, d) $\Delta h = 2d$ [5]

It was clearly shown in Figs. 1a, 2a and 3a, illustrating the flows in the mixing vessel equipped with two impellers located at the spacing of $\Delta h = (0.5 \div 0.7) \cdot d$.

In case of dual impeller sets with the lower PBT-6 or HE-3 impeller, the impact of the upper disc turbine is so intense that the lower impeller ejects the liquid radially towards the vessel's wall. While it should induce an axial flow of liquid, taking into consideration its position inside the mixing vessel. In the case of HE-3 impeller, this trend also occurs at greater spacing. It is evident even when $\Delta h = d$. It is different, however, in case of the set with lower A-315 impeller, which induces an intensive axial flow of liquid, directed towards the bottom of the tank, even at a position close to the upper impeller. When the impeller spacing is being increased, a gradual loss of the interaction between the adjacent

liquid streams can be observed, with simultaneous change of the geometry of circulation loops. In case the lower impeller is PBT-6 turbine or A-315, the loops are being spread along the height of the vessel, and for the dual set with the lower impeller of HE-3 type, additionally, a complete change of the geometry of loops and their position in the tank can be noticed.

3.2. Circulation flow rate of liquid

The liquid flow rate Q_C refers to the motion of liquid in the entire volume of the mixing vessel. It is defined as the stream of liquid flowing through the surface, which is located at any cross-section in the tank. Whereby it is considered, both the axial flow rate Q_z, occurring at the horizontal section plane of the tank, at the height of z_i and the radial flow rate Q_r – present at the vertical section plane, at the radius of r_i. Moreover, assuming the circular symmetry of the flow, they are defined as [9]:

$$Q_z(z_i) = \iint_{S_{z_i}} (\bar{u}_z)_{z_i} \, \mathrm{d}S_{z_i} \tag{2}$$

$$Q_r(r_i) = \iint_{S_{r_i}} (\bar{u}_r)_{r_i} \, \mathrm{d}S_{r_i} \tag{3}$$

Furthermore, assuming axial symmetry, the circulation flow rate of liquid in the mixing vessel, Q_C is equal to the maximum value of the flow rates Q_z and Q_r [10]:

$$Q_C = \max\{|Q_z|, |Q_r|\} \tag{4}$$

The circulation flow rate was calculated on the basis of the components of mean velocity of liquid, evaluated at selected measurement points (Figs. 1÷3).

The quantity and limits of the circulation zones were evaluated on the basis of distributions of resultants of the mean velocity components: radial and axial. The analysis of directions and senses of the mean velocity resultants allowed to evaluate the limits of each zone, by determining the value of z_o height, in around which the real limit of zone can be found. It is exemplified in Fig. 4, where the limits of the respective zones are defined as $z_{o1\text{-}2}$, $z_{o2\text{-}3}$ and $z_{o3\text{-}4}$. The values of the axial components of the mean liquid velocity, measured at the points located the closest to the height coordinate of z_o, just below and above it, were then approximated using a continuous function. Next, it was found by means of standard mathematical procedure that the z value of the height at which this velocity component changed its sign reaching zero.

Thus, the z_g coordinate value of the point on the limit line was obtained, corresponding to a given radius of r. This procedure was repeated for each group of points corresponding to different values of the radius, which was changed every 5 mm. The determination of the limit line, described by the $z_{og} = f(r)$, was based on the approximation of the evaluated z_g values, with usage of the continuous function.

In case the centres of loops (restricted in the respective circulation zones) did not coincide the one straight line corresponding to a certain radius value and parallel to the vessel's axis, it was not possible to evaluate the position of the points of limits, based on

the $\bar{u}_z = f(z)$ function. The vectors of the axial component of the mean velocity took the same sense, near the limit of adjacent circulation zones. In such cases, the points of limit were evaluated using the $\bar{u}_r = f(r)$ function and searching for its zero value corresponding to a certain r argument. This function describes alterations of the radial component of the mean velocity versus the radius, at different heights. Then, the points of the circulation zone limit were described using the *rog* radius, which differed depending on the height in the mixing vessel, replacing the dependency of $z_{og} = f(r)$ – with the $r_{og} = f(z)$ function. The circulation flow rate of liquid was evaluated within the limits of each such determined zone. The equations (2), (3) were converted to following form:

$$Q_z(z_i) = 2\pi \int_{r_1}^{r_2} (\bar{u}_z)_{z_i} \, r \, \mathrm{d}r \tag{5}$$

$$Q_r(r_i) = 2\pi r_i \int_{z_{og1}}^{z_{og2}} (\bar{u}_r)_{r_i} \, \mathrm{d}z \tag{6}$$

The procedure described above was illustrated in Fig. 4a. The profiles of $\bar{u}_r$ velocity component drawn along the vessel's height are marked in this figure, for the four selected radiuses, against the real limits of the considered liquid circulation zone. The area covered by this zone is also marked in Fig. 4b, illustrating the mean radial-axial flow of liquid.
In this case, the $\bar{u}_r$ velocity profiles were integrated using the equation (6), within the limits of zone of $|z_{og1\text{-}2}, z_{og2\text{-}3}|$ corresponding to a given radius of the vessel. The liquid flow within the circulation zone was assumed as in closed-circuit. For each velocity profile, there is some part of it in accordance with the direction of coordinate system ($\bar{u}_r^{(+)}$), and its remaining part is opposite of the coordinate system ($\bar{u}_r^{(-)}$). Thus, the two integrals: $Q_r^{(+)}$ and $Q_r^{(-)}$ were calculated. This procedure was repeated for the further values of *ri* radius, and next, all of obtained values were approximated at the end with usage of the continuous function. Similarly, the procedure was carried out using the equation (5). The maximum of these values was the wanted circulation flow rate Q_{Ci}, of the *i*-th zone in the vessel. The liquid flow rate circulating in the total volume of the vessel was evaluated as the sum of the *n* – flow rates from the respective *n*-zones of circulation, which form the total structure of the flow:

$$Q_{C\,\mathrm{sum}} = \sum_{i=1}^{n} Q_{Ci} \tag{7}$$

Finally, it was presented in the form of a dimensionless circulation flow number, of which values were collected in Table 1 and shown in Fig. 5:

$$K_C = \frac{Q_{C\,\mathrm{sum}}}{n \cdot d^3} \tag{8}$$

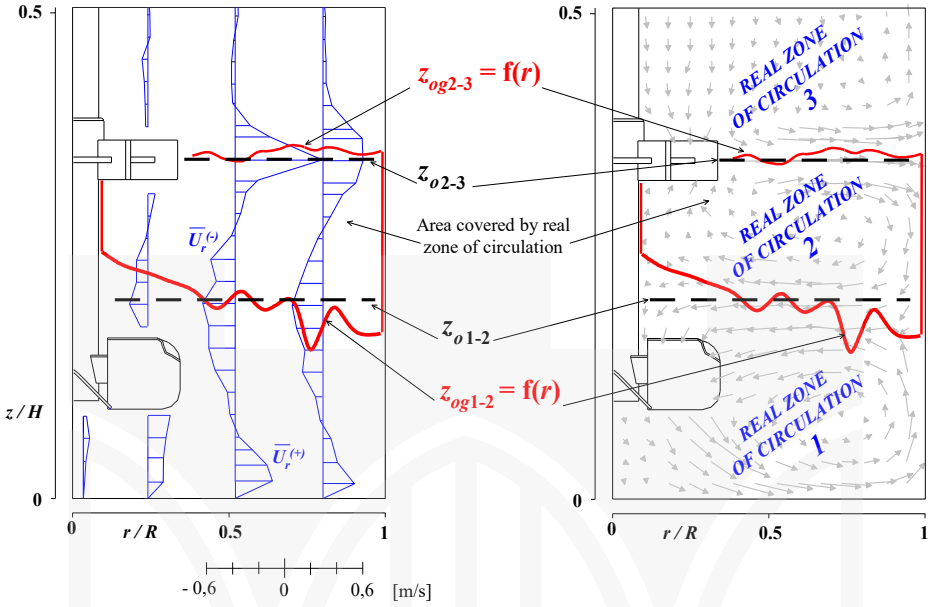

Fig. 4. The location of points of limit z_{og} along the radius of tank. The z_o heights and the real limiting lines of the circulation zones, determined by the procedure of approximation of points z_{og}. The dual impeller set: TR-6 and A-315, $\Delta h = d$

The greatest values of the circulation flow number can be found for the dual set with A-315 impeller. The set with a pitched blade turbine can induce even a more efficient circulation only at the greatest possible impeller spacing. For the values of $\Delta h \geq d$, the least intense circulation is always induced by the set of lower HE-3 impeller. For each of the examined pair of impellers, the circulation flow rate of liquid takes the greatest values when the impellers are spaced by $\Delta h = 1.5d$.

Table 1

The circulation flow numbers of liquid K_C and $K_{C\,calk}$ for the examined dual impellers, with the upper TR-6 disc turbine

Lower impeller:	PTB-6		A-315		HE-3	
	K_C	$K_{C\,calk}$	K_C	$K_{C\,calk}$	K_C	$K_{C\,calk}$
$\Delta h \cong 0.5d$	2.12	2.93	2.28	3.13	2.15	3.00
$\Delta h = d$	3.09	4.69	3.21	4.53	1.93	3.00
$\Delta h = 1.5d$	3.58	5.19	3.63	4.96	3.08	3.98
$\Delta h = 2d$	3.42	4.57	3.22	4.50	2.83	3.88

The analysis of the flow structure was carried out using the Compartment Model Approach (CMA) [7, 8, 13]. For the flow modelling purposes, the real circulation flows of liquid, determined by the radial and axial components of the mean velocity, were replaced

with the contractual circulation compartments: of the first order - situated above and below each impeller, of the second order – in other zones of the vessel. Thus, the zones of liquid circulation (illustrated in Figs. 1÷3) could be presented in the form of contractual, two-dimensional and rectangular compartments specified in the vertical section of the vessel and located cascaded – one above the other. The compartments illustrate the secondary radial-axial circulation flow of liquid in the dual mixing vessel [7, 17, 18]. The limits of these compartments result from the real limits of the circulation zones, z_{og}. The liquid flow inside the compartment is determined by the Q_{Ci} flow rate. The momentum exchange between adjacent compartments takes place at their limiting line, only in the axial direction. It is correlated to the exchange flow rate, induced by the axial component of fluctuation velocity. This component was determined at the points located on the limiting line of the adjacent circulation zones. The values of u'_z, measured at the points located at certain radius coordinate and at several height coordinates, the closest to the corresponding point of the limiting line, z_g, were compiled as a function of the vessel's height and approximated using the continuous function $u'_z = f(z)$. When this function was known, the value of $u'_{zg} = f(z = z_g)$ could be determined. The RMS values, referred to the axial components of fluctuations of the instantaneous velocity, were assumed in place of the u_z' and u_{zg}'. The RMS values were directly obtained from the LDA measurements.

Then, the liquid velocity components, as a function of radius in the vessel, were processed by another approximation using the $u_{zg}' = f(r)$ relationship. This was carried out in the total volume of the dual mixing vessel, at all of the limits which separate corresponding compartments of the circulation flows. The Q_{Ei} flow rate between the adjacent circulation compartments of liquid was determined by the integration process of the $u_{zg}' = f(r)$ function, within the range of r_g radius values. Due to the symmetry of structure and the continuity of flow, it is assumed that the exchange flow occurs in both directions and is equal from both sides as is:

$$Q_{Ei} = 0.5\left[2\pi \int_{r_{g1}}^{r_{g2}} \left[u'_{zg}(r)\right] r \, \mathrm{d}r\right] \tag{9}$$

The total exchange flow rate $Q_{E\,sum}$ was then defined as a sum of all flows determined on the limiting lines between respective compartments of the circulating liquid:

$$Q_{E\,sum} = \sum_{i=1}^{n} Q_{Ei} \tag{10}$$

Thus, the total, corrected liquid flow rate in the dual mixing vessel $Q_{C\,calk}$ was defined as:

$$Q_{C\,cala} = Q_{C\,\mathrm{sum}} + Q_{E\,\mathrm{sum}} \tag{11}$$

and was presented in the dimensionless form, as the corrected, total flow rate number $K_{c\,calk}$:

$$K_{C\,calk} = \frac{Q_{C\,sum} + Q_{E\,sum}}{n\,d^3} \tag{12}$$

Its values, obtained for the examined dual impeller sets, are collected in Table 1 and shown in Fig. 5.

The corrected flow rate of liquid includes the mean flows within the limits of its circulation compartments, as well as the fluctuation flows – between them. It describes the liquid flow, as if it was an averaged inside each compartment, but considered as instantaneous at its limits. The exchange flows cause quantitative increase of the total flow rate of liquid in the vessel, depending on the total value of flow rate – $Q_{E\,sum}$. This value of flow rate is as various as miscellaneous are the flow structures, in dual mixing vessel.

The results indicate that for the impeller spacing of $\Delta h \geq d$ the greatest values of flow rate number $K_{C\,calk}$ can be found if the lower is pitched blade turbine (PBT-6). Slightly less value (by 1÷4%) can be found if it is A-315 impeller. On the other hand, $K_{C\,calk}$ reaches by far the lowest values in case of HE-3 impeller. The situation is different at close location of the impellers ($\Delta h = d$). Then, the $K_{C\,calk}$ number takes the greatest value for the set of lower A-315 impeller, and is of a few percent lower in case of the rest of examined sets.

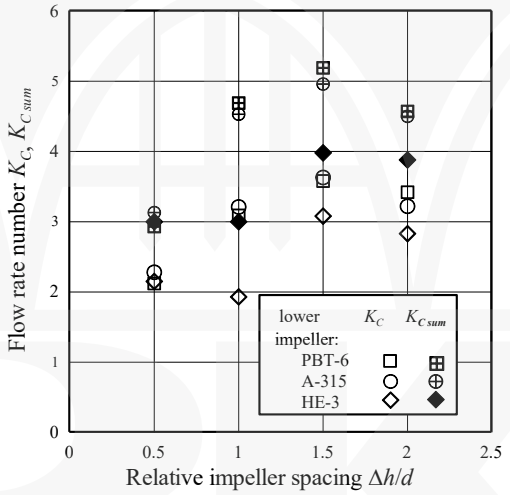

Fig. 5. The flow rate numbers of liquid, K_C and $K_{C\,calk}$ in the dual mixing vessel, versus the relative value of impeller spacing

3.3. Cycle of liquid transport

The flow of liquid is a crucial problem for its mixing. It is related to the transport of liquid elements along the vessel's height, towards the liquid level and reversely. It is possible to describe the liquid transport phenomena in a dual mixing vessel using the assumptions of the CMA model, in the context of momentum exchange within the compartments and between them. The liquid element is successively being moved through the circulation compartments with the velocities of $\bar{u}_r$ and $\bar{u}_z$, and while crossing the compartments' limits, is moving with the velocities of u'_z. An exemplary chart of the trajectories of liquid element is presented in Fig. 6.

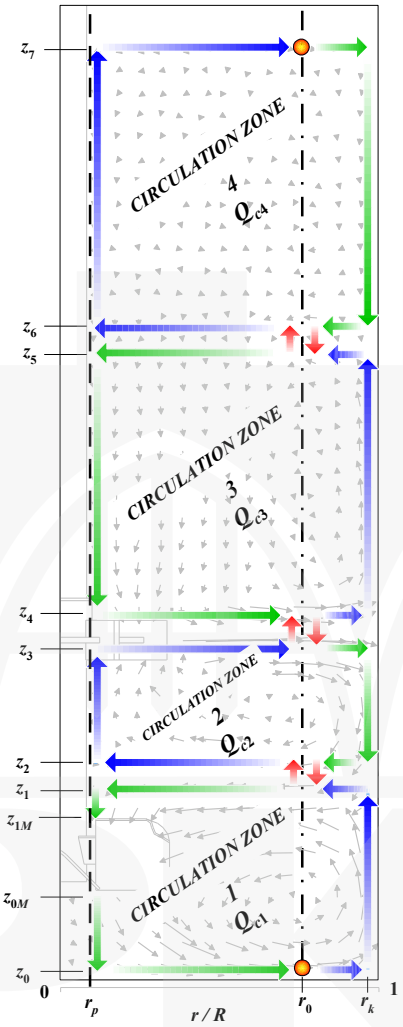

Fig. 6. The chart of liquid element transport in the dual mixing vessel with the lower A-315 impeller and four circulation zones, at $\Delta h = 1d$

Let us assume that the liquid element flows rectilinearly through each length. This element begins its move at the point of coordinates of (r_0, z_0) and flows upward, in the range of [z_0, z_7] and of [r_p, r_k], along the height and radius of the vessel. Once the element reaches one of the above limit coordinates, it changes its direction. Within the compartment, the liquid element flows on the horizontal lengths with the velocity of $\bar{u}_r$, while on the vertical lengths – with the velocity of $\bar{u}_z$. The liquid element traverses each length with different mean velocities. The lengths of element trajectories are set so that they coincide the lines of measurement points, at the middle vertical plane of the vessel. The liquid element crosses the limits of compartments at the points of radial coordinate of r_0, in

which the centres of circulation loops are also located. The crossing velocity of liquid element at these points is u'_z. The calculations were performed for the sets of impellers spaced at $\Delta h = 2d$. The flow structure induced in the mixing vessel, presented in Fig. 6, consists of three compartments of the first order and the fourth – of the second order. The mean velocity values, obtained at the measurement points, were compiled and described with continuous functions, within the respective range: from r_p to r_k and from z_0 to z_7, determining the trajectory of the liquid element. These functions were obtained by the interpolation of discrete values of the velocity, using the MATLAB software and selecting the spline type functions. Thus, to obtain the total transport time of liquid element at the certain length, the numerical integration of the formulas of inversed velocity was performed, according to the equations (13) and (14):

$$\vartheta_j = \int_r \frac{1}{\mathrm{f}_j(r)}\,\mathrm{d}r \tag{13}$$

$$\vartheta_j = \int_z \frac{1}{\mathrm{f}_j(z)}\,\mathrm{d}z \tag{14}$$

where the j-th index refers to the serial number of function, as shown in Table 2.

Table 2

The summary of the functions of liquid element velocity and their intervals of validity (domains)

Lp.	$\bar{u}_i$	r, z
1	$\mathrm{f}_1 = \bar{u}_r(r)$	$r \in \{[r_0, r_k]\} z_0$
2	$\mathrm{f}_2 = \bar{u}_z(z)$	$z \in \{[z_0, z_1]\} r_k$
3	$\mathrm{f}_3 = \bar{u}_r(r)$	$r \in \{[r_k, r_0]\} z_1$
4	$\mathrm{f}_4 = u'_{z1\text{-}2}(z)$	$z \in \{[z_1, z_2]\} r_0$
5	$\mathrm{f}_5 = \bar{u}_r(r)$	$r \in \{[r_0, r_p]\} z_2$
6	$\mathrm{f}_6 = \bar{u}_z(z)$	$z \in \{[z_2, z_3]\} r_p$
7	$\mathrm{f}_7 = \bar{u}_r(r)$	$r \in \{[r_p, r_0]\} z_3$
8	$\mathrm{f}_8 = u'_{z\,2\text{-}3}(z)$	$z \in \{[z_3, z_4]\} r_0$
9	$\mathrm{f}_9 = \bar{u}_r(r)$	$r \in \{[r_0, r_k]\} z_4$
10	$\mathrm{f}_{10} = \bar{u}_z(z)$	$z \in \{[z_4, z_5]\} r_k$
11	$\mathrm{f}_{11} = \bar{u}_r(r)$	$r \in \{[r_k, r_0]\} z_5$
12	$\mathrm{f}_{12} = u'_{z\,3\text{-}4}(z)$	$z \in \{[z_5, z_6]\} r_0$
13	$\mathrm{f}_{13} = \bar{u}_r(r)$	$r \in \{[r_0, r_p]\} z_6$
14	$\mathrm{f}_{14} = \bar{u}_z(z)$	$z \in \{[z_6, z_7]\} r_p$
15	$\mathrm{f}_{15} = \bar{u}_r(r)$	$r \in \{[r_p, r_0]\} z_7$

The numerical integration was performed using the Gaussian quadrature method, and next based on the Newton-Cotes formulas, yielding thereby an exact result of calculations. This way, the functions describing alterations of the radial and axial component of the mean velocity depending on the radius – $\bar{u}_r(r)$ and the vessel's height – $\bar{u}_z(z)$ were obtained. These functions and their intervals were shown in Table 2.

In case the liquid element flowed through the compartments with the velocity values of u'_z, expressed by f_4, f_8 and f_{12} functions, it was assumed that the lengths of $|z_1, z_2|$, $|z_3, z_4|$, $|z_5, z_6|$ were close to zero because the horizontal lengths of the element's trajectory should be located as close to the limits of the adjacent compartments. Therefore, the liquid transport on these lengths could be approximately considered as a pulsing movement, occurring on an infinitely short path, and therefore f_4, f_8, f_{12} functions can be expressed using the limit of a function:

$$\vartheta_j = \lim \frac{z}{\mathrm{f}(u'_z)} \tag{15}$$

These intervals were evaluated considering the most adverse case, the greatest vertical and horizontal flow lengths of the liquid element. Thus, it was stated that the values of r_p and r_k were located as close to the impeller's shaft and the vessel's wall, but far enough, so that neither the boundary layer nor the rotation of the shaft influenced the velocity of the liquid element. Similarly, the values of z_0 and z_7 of height were located as close to the vessel's bottom and to the liquid level, so that the boundary layer and the disturbances on a free liquid surface did not influence the element's velocity.

The duration of cycle of liquid transport was expressed as: $\sum_{j=1}^{m} \vartheta_j$, or in the dimensionless form, as:

$$\Theta = \left(\sum_{j=1}^{m} \vartheta_j \right) \cdot n \tag{16}$$

where m – superscript is the number of lengths (the intervals of integration), which were being traversed by the liquid element while transporting in the tank, wherein: $\{\vartheta_4, \vartheta_8, \vartheta_{12}\} \approx 0$. The results were summarised in Table 3. The energy consumption E during the cycle was also added there.

Table 3

The magnitudes relating to the cycle of liquid transport for the examined dual impeller sets

Lower impeller:	PTB-6			A-315			HE-3		
	$\sum_{j=1}^{m} \vartheta_j$ s	Θ –	E J	$\sum_{j=1}^{m} \vartheta_j$ s	Θ –	E J	$\sum_{j=1}^{m} \vartheta_j$ s	Θ –	E J
$\Delta h = 2 \cdot d$	19.32	96.6	138.1	21.67	108.4	153.4	37.20	186.0	199.8

4. Conclusions and final remarks

If taking into account the mean liquid flow, the application of the disc turbine combined with the axial impeller yields the beneficial effect of mixing. However, it depends on the design of the lower impeller.

The liquid flow rate in the mixing vessel varies, depending on the relative location of the impellers. The change of the impeller spacing affects the change in the flow structure, which can take different transitional forms as well as thoroughly deformed shapes. In such cases, local reinforcing or suppressing of the liquid streams can occur. It can be seen by an increase or decrease of the K_{ccalk} number. There is the exchange flow rate, occurring on the limit of the respective, adjacent compartments. It was expressed as a function of the axial component of fluctuating velocity. The greatest intensity of the induced liquid flow and beneficial energy consumption can be found for the set of the lower PBT-6 turbine. This magnitude is only slightly lower for the set of A-315 impeller. The situation becomes reversed only at a very close position of the impellers.

Nomenclature

d – impeller diameter, m;
D – vessel diameter, m;
H – lower impeller's clearance in vessel, m;
Δh – impeller spacing, m;
K_C – circulation flow number in total liquid volume;
$K_{C\,calk}$ – corrected flow rate number;
n – rotation frequency of impellers, s^{-1};
Q_C – liquid flow rate general, m^3/s;
$Q_{C\,sum}$ – liquid flow rate in total volume of vessel, m^3/s;
$Q_{C\,calk}$ – liquid flow rate corrected, m^3/s;
Q_E – exchange flow rate of liquid in mixing vessel, general, m^3/s;
$Q_{E\,sum}$ – exchange flow rate of liquid in mixing vessel, total, m^3/s;
Q_r – circulation flow rate in radial direction, within circulation zone, m^3/s;
Q_z – circulation flow rate in axial direction, within circulation zone, m^3/s;
r – radius coordinate, m;
R – vessel diameter, m;
Re – Reynolds number for mixing, –;
R – variable and radial coordinate in vessel, m;
Δt – time residence of liquid in the measuring, s;
u'_{zg} – axial component of fluctuation velocity, at point on limiting line, z_{og}, m/s;
$\bar{u}$, $\bar{u}(t)$ – mean liquid velocity, m/s;
Z – variable and axial coordinate in vessel, m;
z – axial coordinate, m;
z_g – real height of points of limit between compartments, height of point of limit, m;
z_o – estimated height of limits between circulation zones, m;
z_{og} – real limit between compartments (circulation zones), m;
ϑ – transport time of liquid element through certain length, s;

Subscripts

i – general index of component, index of summation;
j – index of summation;
r – index of radial component;
z – index of axial component;

Superscripts

(+) – just drawdown;
(–) – refers to the gas-liquid system conditions;

References

[1] Alves S. S., Maia C. I., Vasconcelos J. M. T., *Experimental and modelling study of gas dispersion in a double turbine stirred tank*, Chemical Engineering Science, vol. 57, 2002, 487-496.

[2] Aubin J., Mavros P., Fletcher D. F., Xuereb C., Bertrand J., *Effect of axial agitator configuration (up-pumping, down-pumping, reverse rotation) on flow patterns generated in stirred vessels*, Transactions of the Institution of Chemical Engineers, vol. 79(A8), 2001, 845-856.

[3] Bader F. G., *Modelling mass transfer and agitator performance in multiturbine fermentors*, Biotechnology and Bioengineering, vol. 30(1), 1987, 37-51.

[4] *Chemineer Bulletin*, Nr 710, homepage: http://www.chemineer.com (date of access: 2008-02-10).

[5] Duda A., *Hydrodynamika mieszania cieczy w aparacie z dwoma mieszadłami*, Rozprawa doktorska, Politechnika Krakowska 2015.

[6] Elsner J. W., Drobniak S., *Metrologia turbulencji przepływów*. *Maszyny Przepływowe*, vol. 18, Wydawnictwo PAN, Wrocław-Warszawa-Kraków 1995.

[7] Fajner D., Magelli F., Pasquali G., *Modelling of non-standard mixers stirred with multiple impellers*, Chemical Engineering Communication, vol. 17, 1982, 285-295.

[8] Jahoda M., Machoň V., *Homogenization of liquids in tanks stirred by multiple impellers*, Chemical Engineering & Technology, vol. 17, 1994, 95-101.

[9] Jaworski Z., Nienow A. W., Koutsakos E., Dyster K. W., Bujalski W., *An LDA study of turbulent flow in a baffled vessel agitated by a pitched blade turbine*, Transactions of the Institution of Chemical Engineers, vol. 69, Part A, 1991, 313-320.

[10] Jaworski Z., Nienow A. W., Dyster K. W., *An LDA study of the turbulent flow field in a baffled vessel agitated by an axial, down-pumping hydrofoil impeller*, Canadian Journal of Chemical Engineering, vol. 74, 1996, 3-15.

[11] Johnson R. W., The *handbook of fluid dynamics*, CRC Press LLC, Boca-Raton, USA, 2000.

[12] *Lightnin Bulletin*, Nr E-120 09/01, homepage: http://www.lightninmixers.com (date of access: 2008-02-15).

[13] Manfredini R. Cavallera V., Marini L., Donati G., *Mixing and oxygen transfer in conventional stirred fermenters*, Biotechnology and Bioengineering, vol. 25(12), 1983, 3115-3131.

[14] MATLAB *Online Documentation*, homepage: http://www.mathworks.com/help/matlab (date of access: 2014-08-03).

[15] Saito F., Nienow A. W., Chatwin S., Moore J. T. J., *Power gas dispersion and homogenisation characteristics of Scaba SRGT and Rushton turbine impellers*, Chemical Engineering Japan, vol. 25(3), 1992, 281-287.

[16] Takenaka K., Takahashi K., Bujalski W., Nienow A. W., Paolini S., Paglianti A., Etchells A. W., *Mixing time for different diameters of impeller at a high solid concentration in an agitated vessel*, Journal of Chemical Engineering of Japan, vol. 38(5), 2005, 309-315.

[17] Vasconcelos J. M. T., Alves S. S., Barata J. M., *Mixing in gas-liquid contractors agitated by multiple turbines*, Chemical Engineering Science, vol. 50(14), 1995, 2343-2354.

[18] Vrábel P., van der Lans R. G. J. M., Luyben K. Ch. A. M., Boon L., Nienow A. W., *Mixing in large-scale vessels stirred with multiple radial or radial and axial up-pumping impellers: modelling and measurements*, Chemical Engineering Science, vol. 55, 2000, 5881-5896.